Electronic Supplementary Information

Coexistence of Magnetic and Electric Orderings in a Divalent Cr^{2+}-Based Multiaxial Molecular Ferroelectric

Yong Ai,[a†] Rong Sun,[b†] Yu-Ling Zeng,[a] Jun-Chao Liu,[a] Yuan-Yuan Tang,[a] Bing-Wu Wang,[b] Zhe-Ming Wang,[b] Song Gao,[*b] and Ren-Gen Xiong[*a]

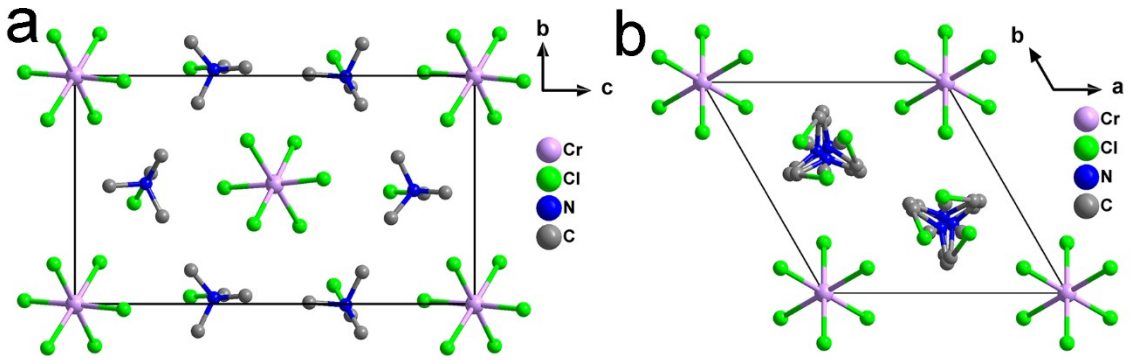

Figure S1. Packing view of crystal structures for TMCM-$CrCl_3$ in (a) LTP and (b) HTP. H atoms were omitted for clarity.

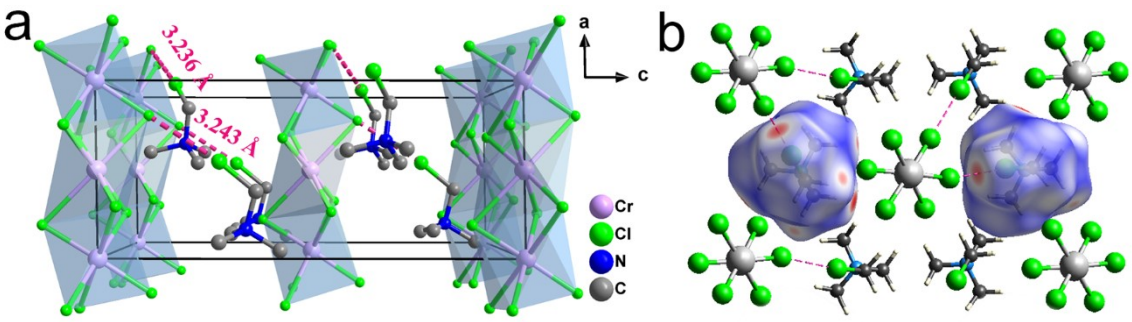

Figure S2. (a) Packing view of crystal structure for TMCM-$CrCl_3$ along *b*-axis in LTP. (b) Hirshfeld d_{norm} surfaces of TMCM cations in TMCM-$CrCl_3$ in LTP. The pink dotted lines represent the C−Cl···Cl−Cr halogen bonds. H atoms were omitted for clarity.

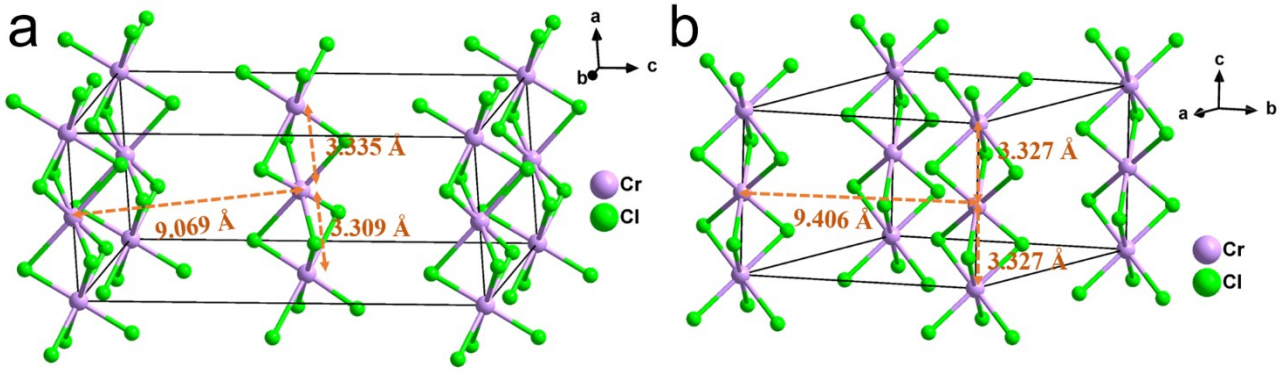

Figure S3. Packing view of crystal structures for TMCM-$CrCl_3$ in (a) LTP and (b) HTP. The brown dashed lines represent the distances between adjacent Cr atoms. TMCM cations were omitted for clarity.

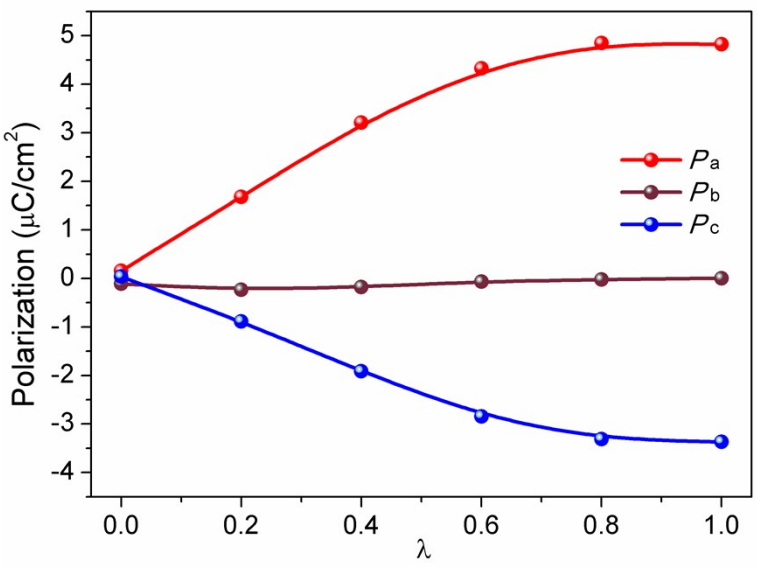

Figure S4. Ferroelectric polarization evolution of TMCM-$CrCl_3$ as a function of structure parameter λ.

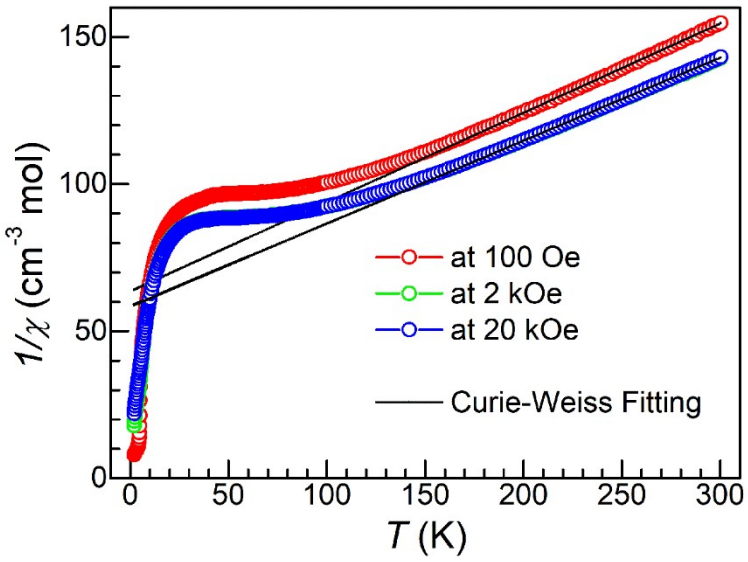

Figure S5. Temperature dependences of 1/χ for TMCM-$CrCl_3$ measured in the temperature range of 2-300 K. The black solid lines are fitted by the Curie-Weiss law.

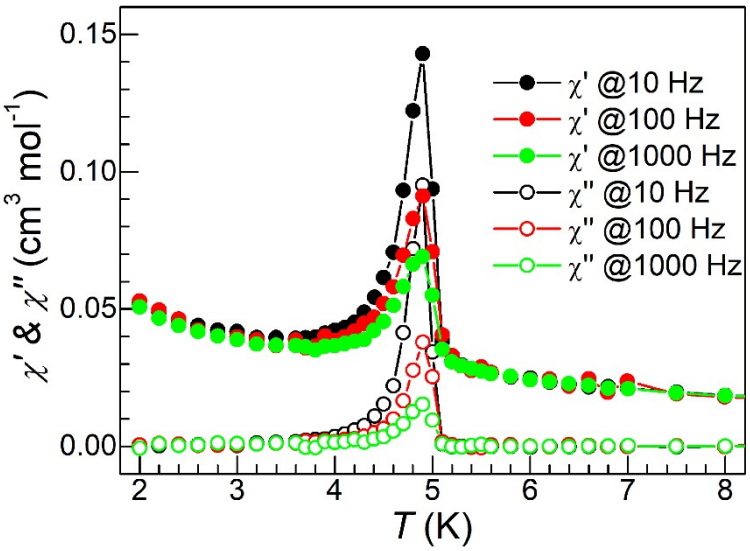

Figure S6. The frequency-independent peaks on ac susceptibilities data for TMCM-$CrCl_3$.

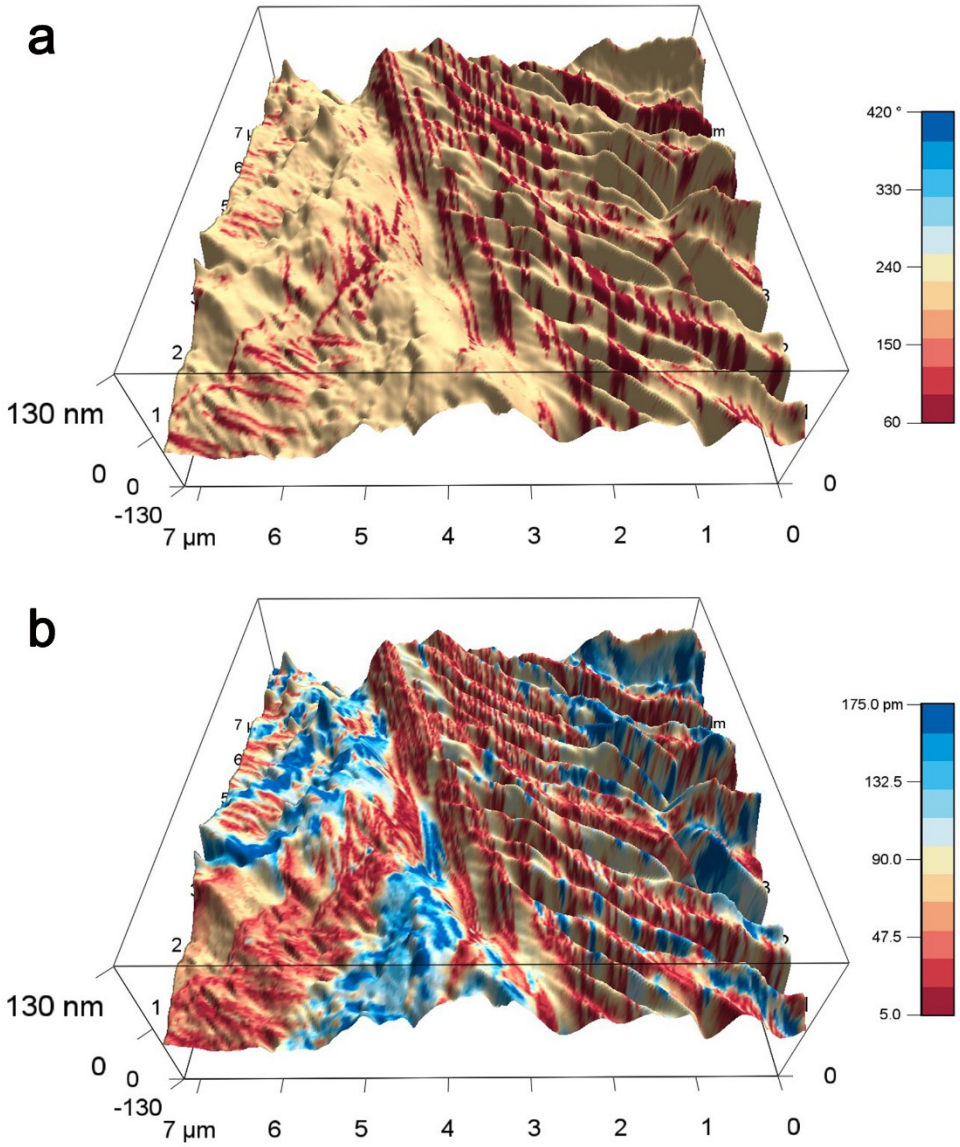

Figure S7. Phase mapping (a) and amplitude mapping (b) of the vertical PFM overlaid on the 3D topography for the thin film of TMCM-$CrCl_3$.

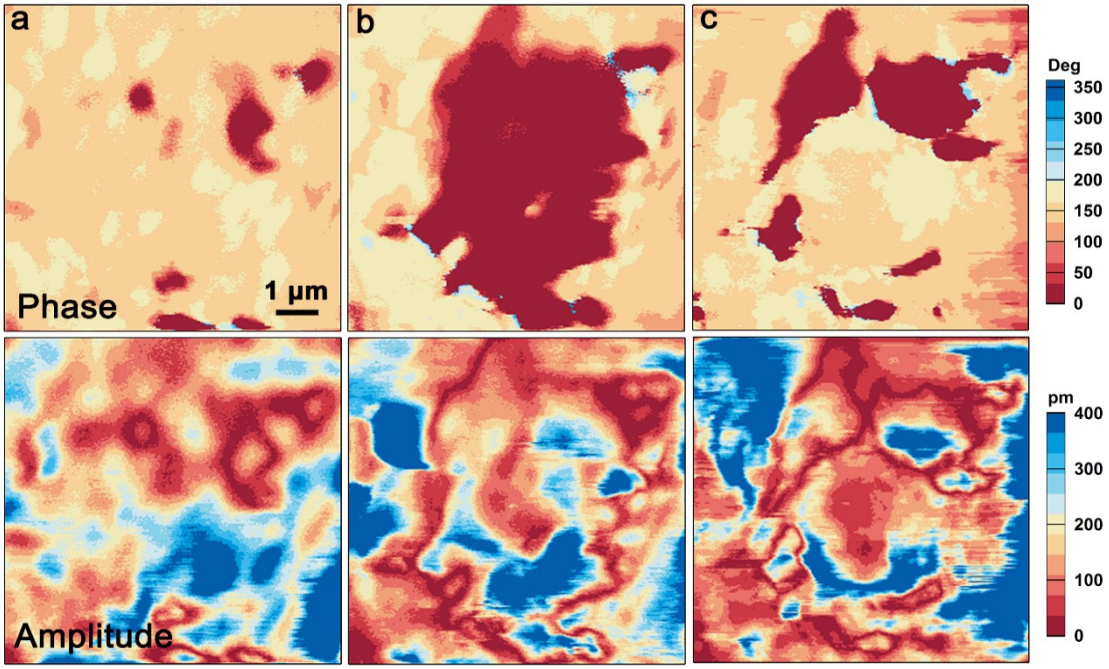

Figure S8. Vertical PFM phase (top) and amplitude (bottom) images of the thin film for TMCM-$CrCl_3$. (a) Initial state. (b) After the first switching with negative bias at -50 V. (c) After the succeeding switching with positive bias at +30 V.

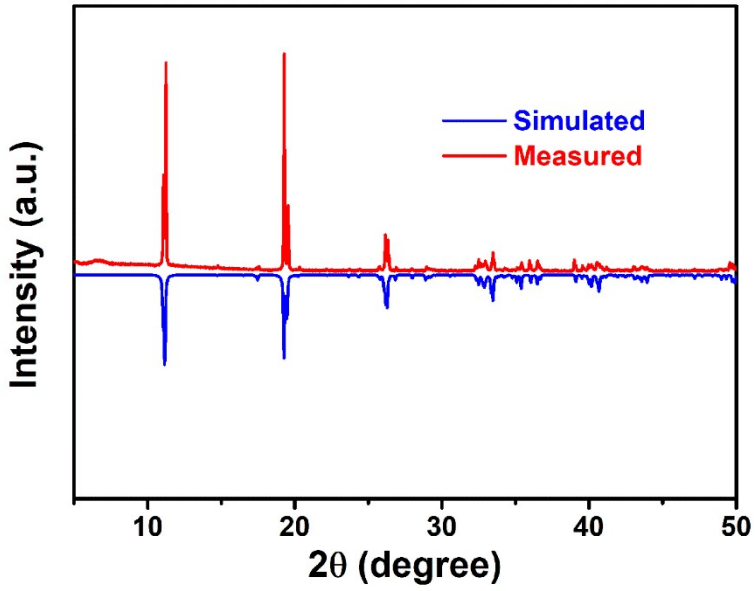

Figure S9. The measured PXRD pattern of TMCM-$CrCl_3$ at 293 K match well with the simulated one from crystal data in LTP, verifying the good phase purity.

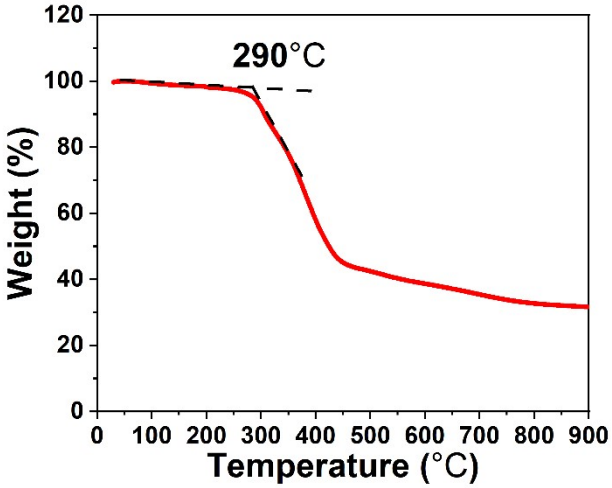

Figure S10. TGA plot of TMCM-$CrCl_3$, measured under nitrogen atmosphere.

Table S1. Crystal data and structure refinement for TMCM-$CrCl_3$.

Compound	**TMCM-$CrCl_3$**	
Formula	$C_4H_{11}ClNCrCl_3$	
Temperature	223 K	415 K
Weight	533.88	266.96
Crystal system	Monoclinic	Hexagonal
Space group	*Pc*	$P6_3/m$
a (Å)	6.6436(7)	9.4058(10)
b (Å)	9.1155(10)	9.4058(10)
c (Å)	16.003(19)	6.6531(8)
α	90	90
β (°)	90.97	90
γ	90	120
V (Å^3)	969.0(12)	509.74(12)
Z	2	2
R_{int}	0.1300	0.0805

R_1	0.0861	0.1247
wR_2	0.2438	0.3474
GOF	1.002	1.006

Table S2. Selected bond lengths [Å] and bond angles [°] for TMCM-$CrCl_3$.

Temperature	**bond lengths [Å] and bond angles [°]**			
223 K	Cr1—Cl1	2.382 (5)	Cr2—Cl6	2.398 (6)
	Cr1—Cl4	2.411 (5)	Cr2—Cl2^{i}	2.467 (5)
	Cr1—Cl3	2.450 (5)	Cr2—Cl3	2.470 (5)
	Cr1—Cl2	2.473 (5)	Cl2—Cr2^{ii}	2.467 (5)
	Cr2—Cl5	2.377 (6)		
	Cl1—Cr1—Cl4	177.6 (2)	Cl5—Cr2—Cl2^{i}	92.48 (19)
	Cl1—Cr1—Cl3	92.49 (16)	Cl6—Cr2—Cl2^{i}	87.16 (18)
	Cl4—Cr1—Cl3	87.83 (19)	Cl5—Cr2—Cl3	87.18 (19)
	Cl1—Cr1—Cl2	87.59 (19)	Cl6—Cr2—Cl3	93.05 (18)
	Cl4—Cr1—Cl2	92.04 (16)	Cl2^{i}—Cr2—Cl3	177.3 (2)
	Cl3—Cr1—Cl2	178.8 (2)	Cr1—Cl3—Cr2	85.37 (16)
	Cl5—Cr2—Cl6	177.4 (2)	Cr2^{ii}—Cl2—Cr1	84.09 (15)
415 K	Cr1—Cl1^{i}	2.552 (5)	Cr1—Cl1^{v}	2.552 (5)
	Cr1—Cl1^{ii}	2.552 (5)	Cr1—Cl1	2.552 (5)
	Cr1—Cl1^{iii}	2.552 (5)	Cl1—Cr1^{vi}	2.552 (5)
	Cr1—Cl1^{iv}	2.552 (5)		

Cl1^{i}—Cr1—Cl1^{ii}	180.0 (4)	Cl1^{iii}—Cr1—Cl1^{v}	82.12 (16)
Cl1^{i}—Cr1—Cl1^{iii}	82.12 (16)	Cl1^{iv}—Cr1—Cl1^{v}	180.0 (4)
Cl1^{ii}—Cr1—Cl1^{iii}	97.88 (16)	Cl1^{i}—Cr1—Cl1	97.88 (16)
Cl1^{i}—Cr1—Cl1^{iv}	97.88 (16)	Cl1^{ii}—Cr1—Cl1	82.12 (16)
Cl1^{ii}—Cr1—Cl1^{iv}	82.12 (16)	Cl1^{iii}—Cr1—Cl1	180.0
Cl1^{iii}—Cr1—Cl1^{iv}	97.88 (16)	Cl1^{iv}—Cr1—Cl1	82.12 (16)
Cl1^{i}—Cr1—Cl1^{v}	82.12 (16)	Cl1^{v}—Cr1—Cl1	97.88 (16)
Cl1^{ii}—Cr1—Cl1^{v}	97.88 (16)	Cr1^{vi}—Cl1—Cr1	81.3 (2)